

# Development of Deep Groove Ball Bearings for High-speed Rotation

Y. TANIGUCHI T. UMENO

*Motors used in hybrid electric vehicles (HEV), electric vehicles (EV), and the like are required to be small and high-output. The downsizing of the motor brings demands for an increase in rotations to preserve motor output, and the need for higher speed in bearings is also increasing. In response to these needs, we have developed a deep groove ball bearing for high-speed rotation which adopts a dual-support type resin cage, which we will introduce in this report.*

**Key Words:** ball bearing, cage, high-speed, dual-support

## 1. Introduction

As high fuel efficiency needs continue to increase, it is predicted that the demand for HEVs and EVs will also continue to grow. The drive motors used in HEVs and EVs are required to be compact and lightweight as they must be installed in limited space. Meanwhile, in order to make a motor smaller at the same time as maintaining high output, there is a need to increase rotational speed therefore a bearing capable of supporting high-speed rotation is necessary for the support bearings of the motor also. This paper introduces the development of a deep groove ball bearing for high-speed rotation.

## 2. Issues Regarding High-Speed Rotation

The drive motors of HEVs and EVs either use oil or grease lubrication, however the former is often used for high-speed rotation. The cage used in a deep groove ball bearing is normally an iron cage or snap cage, however in cases where the bearing is used at high-speed rotation with oil lubrication, the allowable rotational speed is often determined by the high-speed limit of the cage. If an iron cage is used, the contact between the balls and cage pocket intensifies at high-speed rotation due to the eccentric motion of the cage and insufficient lubrication at the contact points will lead to seizure between the balls and cage. **Figure 1** shows the state of an iron cage after a high-speed rotation test.

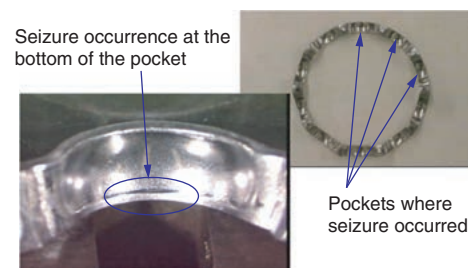


**Fig. 1** State of iron cage after high-speed test

Meanwhile, in the case of a snap cage, the pocket claws are susceptible to deformation due to the centrifugal force generated by the single-support type and although the snap cage has superior high-speed performance compared to an iron cage, when used under high-speed rotation conditions, temperature may increase due to strong contact between the balls and pocket claws as a result of deformation, which would result in seizure. **Figure 2** shows the state of a snap cage after a high-speed rotation test.



**Fig. 2** State of snap cage after high-speed test

To make snap cages more suited for high-speed applications by minimizing deformation caused by centrifugal force, a conventional measure of making the annular portion of the cage thicker in the axial direction can be implemented to enhance rigidity. However, even in cages with enhanced rigidity, the deformation of the claws is significantly large at a high-speed rotation whereby the  $d_m n$  value\*1 exceeds 1 500 000  $d_m n$  and temperature increases due to strong contact between the balls and pocket claws, thus resulting in seizure.

Considering this, the only way to increase a snap cage’s ability to accommodate high-speed would be to change the shape of the cage to minimize deformation at high-speed rotation.

\*1  $d_m n$  value: Bearing P.C.D. × rotational speed  
(mm) (min<sup>-1</sup>)

### 3. Features of the Developed Cage

On this occasion, we have developed a dual-support type cage consisting of two snap cages of identical shapes combined as a single set (Fig. 3).

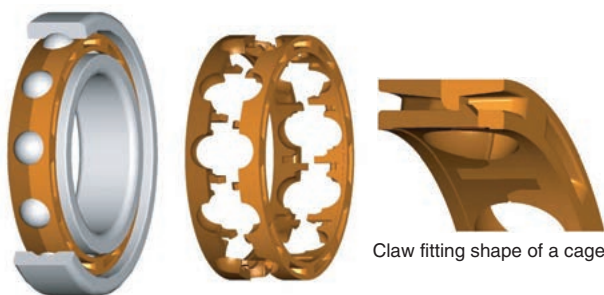


Fig. 3 Developed cage

The dual-support configuration minimizes any deformation caused by centrifugal force.

Moreover, even in regards to the shape of the claws in the combined portion, by forming the claws from the inside, the shape is less susceptible to deformation by centrifugal force. We performed an FEM analysis of cage deformation to verify the effects of deformation reduction in the developed cage. Table 1 shows the analyzed cages, Table 2 shows the analysis conditions and Fig. 4 shows the analysis results.

Table 1 Analyzed cages

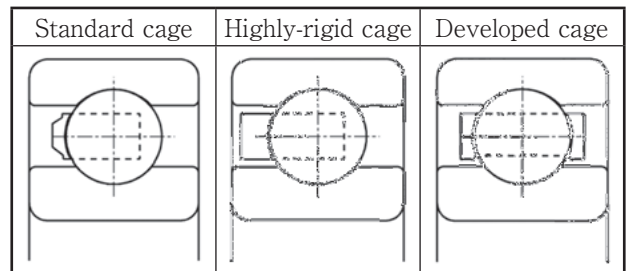


Table 2 Analysis conditions

Bearing number	6007 (I.D. $\phi 35 \times$ O.D. $\phi 62 \times$ Width 14)
Rotational speed, min <sup>-1</sup>	MAX. 50 000
Temperature, °C	120

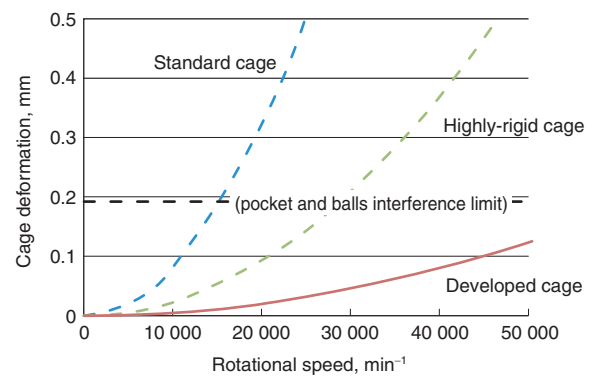


Fig. 4 Analysis results

The analysis results of Fig. 4 show that, compared to a standard cage, the highly-rigid cage with a thicker annular portion in the axial direction has less deformation however, as mentioned above, its interference limit with the bearing balls is reached at speeds in excess of 30 000 min<sup>-1</sup> ( $d_m n$  value: Approx. 1 500 000).

In comparison, the developed cage has even less deformation than the highly-rigid cage and does not interfere with the bearing balls even at speeds of 40 000 min<sup>-1</sup> ( $d_m n$  value: Approx. 2 000 000).

## 4. Evaluation

### 4.1 Cage

#### (1) Fatigue strength

We conducted an experiment to verify the fatigue strength of the developed cage. Moreover, for the resin cage, we also confirmed the fatigue strength of a cage after it had been dipped in oil as strength decreases due to deterioration from use in oil lubrication. Table 3

shows the test conditions, **Table 4** shows the oil dipping conditions and **Fig. 5** shows the test equipment. The load on the cage was applied in the tensile direction between two pin-shaped fixtures by moving the pin-shaped fixture on the rotating ring side in the rotational direction. Tests were conducted at various loads until the cage broke and the number of repetitions was confirmed.

**Table 3** Test conditions

Sample, cage	New cage/oil-dipped cage
Frequency, Hz	10
Ambient temperature, °C	20 ± 5 (normal temperature)

**Table 4** Oil dipping conditions

Oil type	ATF
Temperature, °C	140
Time, h	500

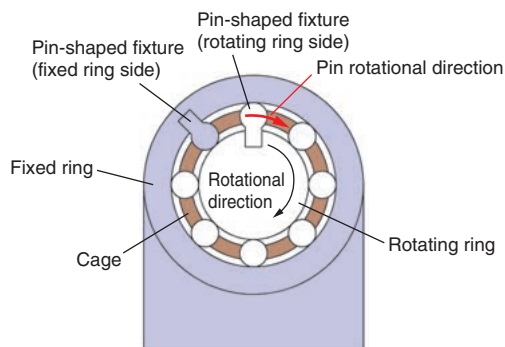


**Fig. 5** Test equipment

**Figure 6** shows the results of a fatigue strength test, while **Fig. 7** is a photo of the cage after a fatigue strength test has been conducted. **Figure 7** shows that the thinnest annular portion of the cage (the back) is broken, therefore we can ascertain that the back is the weakest portion. The stress occurring on the vertical axis shown in **Fig. 6** is the stress of the back calculated through FEM analysis from the applied load.

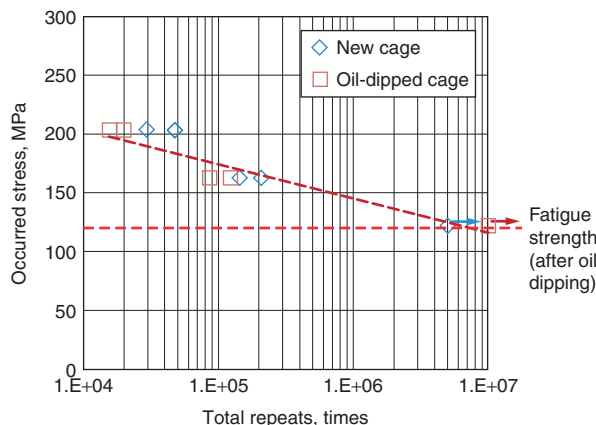


**Fig. 6** Fatigue strength test results

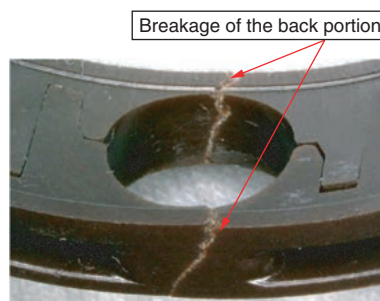


**Fig. 7** Cage after fatigue strength test

**Figure 8** shows the results of an analysis to verify the stress occurring on the developed cage at a speed of 40 000 min<sup>-1</sup> ( $d_{mn}$  value: Approx. 2 000 000) and these results reveal that the occurred stress is smaller than the fatigue strength after oil dipping even under such high-speed conditions.

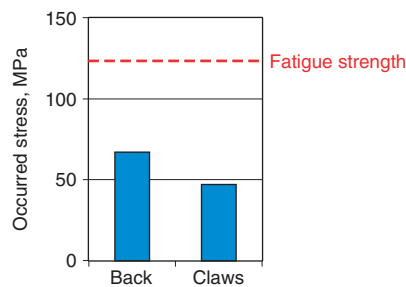


**Fig. 8** Results of occurred stress analysis

(2)Heat shock test

A heat shock test was conducted for the developed cage in order to confirm how much it was affected by heat shock. **Table 5** shows the test conditions. No abnormalities such as deformation or splits were observed in the cage after the test was carried out.

**Table 5** Test conditions

Test pattern	
Number of cycles	200

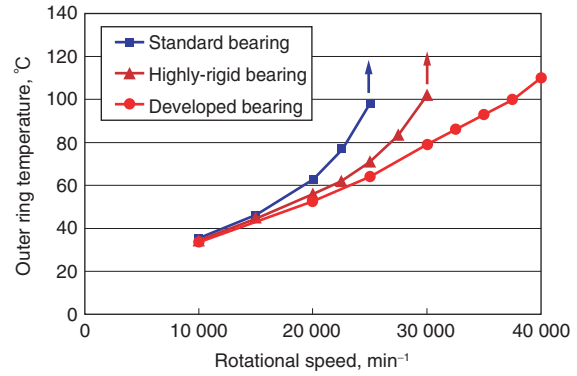


**Fig. 10** Results of high-speed performance evaluation

**4. 2 Bearing**

(1)High-speed performance

A comparison was made of the temperature increase in bearings fitted with the existing cages (standard cage, highly-rigid cage) and the developed cage. **Table 6** shows the test conditions, **Fig. 9** shows the test equipment and **Fig. 10** shows the test results. The upward-pointing arrows in **Fig. 10** for rotational speed indicate that an abnormal temperature increase would occur at rotational speeds any higher than the one given. Abnormal temperature increase did not occur on the developed cage even at a speed of 40 000 min<sup>-1</sup>, proving it had a high-speed performance more than 1.3 times higher than that of the highly-rigid cage (30 000 min<sup>-1</sup>.)

**Table 6** Test conditions

Bearing number	6007 (I.D. $\phi 35 \times$ O.D. $\phi 62 \times$ Width 14)
Radial load, N	1 600
Axial load, N	0
Oil supply method	Oil drip lubrication
Oil type	ATF
Oil temperature	Normal temperature (natural temperature rise)
Oil amount, ml/min	5

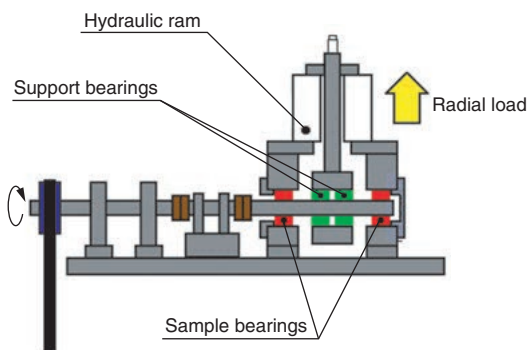


**Fig. 9** Test equipment

(2)Durability

①High-speed durability

A high-speed durability test was performed for the developed cage. **Table 7** shows the test conditions. The results of the test showed the developed cage satisfied the test condition of 200 hours. **Figure 11** shows the external appearance after the test was performed and from this it is clear that there was no flaking or seizure and no abnormalities such as wear on the cage either.

**Table 7** Test conditions

Bearing number	6007 (I.D. $\phi 35 \times$ O.D. $\phi 62 \times$ Width 14)
Radial load, N	1 600
Axial load, N	0
Rotational speed, min <sup>-1</sup>	30 000
Oil supply method	Oil drip lubrication
Oil type	ATF
Oil temperature, °C	140
Oil amount, ml/min	50
Test time, h	200

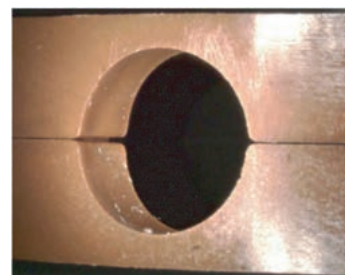


**Fig. 11** Appearance after high-speed durability test

②High-load durability

A high-load durability test was performed for the developed cage. **Table 8** shows the test conditions. An oil-dipped cage was used. Both of the developed cages tested satisfied the condition of three times the calculated life (**Fig. 12**). **Figure 13** shows the external appearance after the test was performed and from this it is clear that there was no flaking or seizure and no abnormalities such as wear on the cage either.

**Table 8** Test conditions

Bearing number	6007 (I.D. $\phi 35 \times$ O.D. $\phi 62 \times$ Width 14)
Cage	Oil-dipped cage (Conditions: <b>Table 4</b> )
Radial load, N	4 900
Axial load, N	0
Rotational speed, min <sup>-1</sup>	10 000
Inclination of shaft	3/1 000
Oil supply method	Oil drip lubrication
Oil type	ATF
Oil temperature, °C	80
Oil amount, ml/min	50
Test time, h	171 (3 times the calculated life)

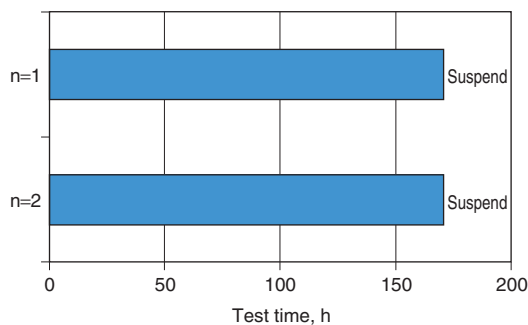


**Fig. 12** High-load durability test results



**Fig. 13** Appearance after high-load durability test

**5. Conclusion**

It was confirmed that the developed cage has a high-speed performance over 1.3 times that of existing cages (standard cage, highly-rigid cage). Moreover, even after heat shock and durability tests, it was confirmed that the developed cage was free of abnormalities and displayed satisfactory durability. In line with the future growth of the HEV and EV markets, it is predicted that motors will become more high-speed. This report introduced a deep groove ball bearing for high-speed rotation however by continuing to engage in the development of new technologies aimed at increasing bearing performance, JTEKT wishes to contribute to better fuel efficiency of automobiles and energy conservation.

**References**

- 1) H. Dodoro, T. Iwata, H. Matsuyama: Tribology Conference Proceedings, 2017 spring Tokyo (2017) D30.
- 2) K. Yokota: Technological Trends and Outlook of Automotive Bearings, JTEKT ENGINEERING JOURNAL, No. 1014E (2017) 14.
- 3) M. Murakami, Y. Takahashi, D. Okamoto: Efforts towards a More Efficient Resin Cage for Ball Bearings, JTEKT ENGINEERING JOURNAL, No. 1011E (2014) 39.



Y. TANIGUCHI \*



T. UMENO \*\*

\* Automotive Bearing Development Dept., Bearing Operations Headquarters

\*\* Experiment & Analysis Dept., Bearing Operations Headquarters